agronomy

MDPI

Article

Evolutionary Trend Analysis of Agricultural Non-Point Source Pollution Load in Chongqing Based on Land Use Simulation

Kangwen Zhu [1,2,*], Yan Zhang [1], Xiaosong Tian [1,3,*], Dongjie Guan [1], Sheng Zhang [2], Yong He [1] and Lilei Zhou [1]

[1] School of Smart City, Chongqing Jiaotong University, Chongqing 400074, China; 622230100014@mails.cqjtu.edu.cn (Y.Z.); 990201100029@cqjtu.edu.cn (D.G.); 990020050408@cqjtu.edu.cn (Y.H.); zhoulleieco2016@cqu.edu.cn (L.Z.)
[2] Chongqing Academy of Eco-Environmental Sciences, Chongqing 401147, China; zs.cqee@gmail.com
[3] School of Resources and Safety Engineering, Chongqing Vocational Institute of Engineering, Chongqing 402260, China
* Correspondence: zhukangwen@cqjtu.edu.cn (K.Z.); tianxs@cqvie.edu.cn (X.T.)

Abstract: Analysis of the relationship between future land use change and agricultural non-point source pollution (ANPSP) evolution is vital to promoting sustainable regional development. By simulating future land use types, we can identify and analyze the evolution trend of ANPSP. This study takes Chongqing as a case study to establish an integrated solution based on the PLUS model, output coefficient model, and GIS technology. The solution can simulate data, identify trends, and identify key control areas under future development scenarios. The results show that the PLUS model can simulate land use types at the provincial scale with high accuracy, with a Kappa coefficient of around 0.9. The land use type changes show that urban expansion has occupied a large amount of cultivated land. From 2000 to 2020, the proportion of high-load areas with TN pollution load levels was 4.93%, 5.02%, and 4.73%, respectively. Under the two scenarios in 2030–2050, the number of high-load areas decreased, and the average load level decreased from west to east. Sensitivity analysis found that risk changes are more sensitive to the increase in fertilizer application. When the TN and TP output coefficients are increased, the number of towns with increased levels is greater than those with decreased levels when the output coefficients are decreased. Sensitivity analysis can better identify key pollution control areas. The areas sensitive to changes in farmers' behavior are mainly the Hechuan District, Nanchuan District, Qijiang District, Jiangjin District, and Bishan District. This study provides data and decision-making support for rural green development and water environment improvement.

Keywords: agricultural non-point source pollution; PLUS model; output coefficient model; sensitivity analysis; Chongqing

Citation: Zhu, K.; Zhang, Y.; Tian, X.; Guan, D.; Zhang, S.; He, Y.; Zhou, L. Evolutionary Trend Analysis of Agricultural Non-Point Source Pollution Load in Chongqing Based on Land Use Simulation. *Agronomy* **2024**, *14*, 737. https://doi.org/10.3390/agronomy14040737

Academic Editor: Shicheng Li

Received: 28 February 2024
Revised: 25 March 2024
Accepted: 28 March 2024
Published: 2 April 2024

1. Introduction

With the rapid development of the agricultural economy and urbanization, the contradiction between economic growth and the ecological environment is becoming increasingly prominent. Excessive pesticides and fertilizers result in the leaching of nitrogen and phosphorus from the soil into surface and groundwater, leading to agricultural non-point source pollution (ANPSP) [1,2]. Wide distribution, multiple sources, continuous emissions, randomness, and potential hazards characterize ANPSP. Quantifying and identifying the pollution load and critical control areas of ANPSP is the key to green development and constructing a beautiful China [3]. As point-source pollution is controlled, ANPSP has become the world's primary source of water pollution, attracting widespread attention from all over the world. For example, in the European Union and Germany, agriculture accounts for about 55% and 48% of surface water pollution, respectively [4]; in Pakistan, due to the unqualified quality of water resources, the concentration of arsenic in groundwater in some areas is too high, causing 40% of deaths and 50% of waterborne infections [5]; in South Korea, 60% of water pollution is related to non-point source pollution from agricultural activities [6]; in China, according to the results of the second national pollution source survey, the total emission of water pollutants in China is about 26.0774 million tons, of which the proportions of COD, TN, and TP emissions from agricultural sources are 49.77%, 46.52%, and 67.22%, respectively [7]. Therefore, an accurate estimation of the pollution load of ANPSP is essential for solving the pollution problem. It is a critical issue that must be addressed in national governance and rural green development in the present and future.

As research on ANPSP deepens, current research hotspots focus on pollution load, mechanism research, prevention techniques, relevant models, risk assessment, and source identification [8,9]. For example, Zhou et al. [10] used the PTRFFM to analyze the agricultural NPS load of Miyun Reservoir and identified areas with high pollutant transmission rates. Yu et al. [11] used the source–sink landscape theory to explore the intensive agricultural watersheds in southeastern China quantitatively and found that the proportion of sink-type landscapes is large. Currently, ANPSP models are mainly based on meteorological data, land use data, and pollution survey data. They generally include AGNPS, AnnAGNPS, HSPF, and SWAT models. These models require a large amount of input data. Due to the differences in data input and the difficulty in obtaining complete and high-precision data in some areas, the accuracy of the models is affected [12]. Currently, there are three main methods for evaluating the pollution load of ANPSP: (1) Small-scale evaluation based on models such as SWAT, such as Zhang et al. [13] used the SWAT model and multiple scenarios to calculate the spatial nitrogen pollution in Luoyang City from 2009 to 2018 and analyze the reasons for the change in nitrogen pollution. (2) Large-scale evaluation based on panel data, such as Wang et al. [14] used panel data from 37 cities in the Yangtze River Delta from 2000 to 2019 to measure ANPSP. (3) Grid-scale evaluation based on the output coefficient method, such as Li et al. [15] used the output coefficient model to evaluate the impact of ANPSP on TN and TP in Beijing, Daqing, and the Three Gorges Reservoir areas. The output coefficient model is also applicable to other countries and regions. Johnes [16] calculated the nitrogen and phosphorus loads in the catchment area of the Windrush River, a tributary of the Thames River in the United Kingdom, using an output coefficient model; Worrall et al. [17] found through an output coefficient model that the release of nitrogen from the soil in the UK is showing a decreasing trend; Zhang et al. [18] simulated the annual variation of phosphorus load in diffusion runoff in Colorado, New York, and Ohio using an output coefficient model. Currently, there is little research on the evolution trend of ANPSP in the future. Zhu et al. [19] used the CLUE-S model to assess the trend of ANPSP risk in the Fuling District of Chongqing, which belongs to the county-level scale research. Overall, there is little research on the trend evaluation of ANPSP load at the provincial scale. Land use simulation is a vital issue that needs to be solved. Currently, common land use-type data simulation methods include CA-Markov models, system dynamics models, CLUE-S models, and PLUS models [20–22]. Blissag et al. [23] simulated land use changes in the HoDNA basin from 2030 to 2050 using the CA-ANN approach; Chasia et al. [24] simulated potential land use changes in the SiO Malaba Malakisi catchment area using the CLUE-S model. Among these models, only the PLUS model is suitable for land use-type data simulation at the provincial scale.

Chongqing is a typical mountain city with a high proportion of mountains, a high proportion of rural areas, a high intensity of land development and utilization, and abundant and concentrated precipitation. As a result, the risk of ANPSP in the region is relatively high. According to publicly available data from Chongqing in 2020, the application intensity of fertilizer per hectare of cultivated land area was 266.36 kg/hm^2, which exceeds the internationally recognized safe upper limit of fertilizer application of 225 kg/hm^2 [25].

Xiao et al. [26] pointed out that from 1998 to 2011, the average annual emissions of TN and TP in the Chongqing section of the Three Gorges Reservoir Area were 134,076.92 t and 61,651.66 t, respectively, with an average emission intensity of 1910 kg/hm^2 and 610 kg/hm^2; Guan et al. [27] pointed out that the ANPSP in various districts and counties of the Three Gorges Reservoir Area is generally at medium risk, with the Nan'an District of Chongqing having the highest risk value, followed by areas such as Dadukou and Shapingba. It is evident that the implementation of ANPSP control in Chongqing is urgent. Chongqing is located in the upper reaches of the Yangtze River and is a critical ecological security barrier zone with important ecological status. The assessment of the ANPSP load under future development scenarios in Chongqing is of great scientific and practical significance for reducing regional pollution risks and promoting regional rural green development.

Therefore, this study takes Chongqing as a case study. First, it simulates Chongqing's land use type data from 2030 to 2050 under the natural development scenario (ND) and the ecological protection scenario (EP) based on the PLUS model. Second, it identifies the evolution patterns and trends of the ANPSP load in Chongqing from 2000 to 2050 based on the output coefficient model. Third, it conducts sensitivity analysis through output coefficient adjustment to analyze the evolution trends of ANPSP load under different fertilization scenarios. Finally, it comprehensively identifies key control areas for ANPSP, providing methods and data support for rural green development and precise pollution control.

2. Materials and Methods

2.1. Study Area

Chongqing is located in southwest China and is at the heart of the Three Gorges Reservoir area, as shown in Figure 1. It is an essential ecological barrier in the upper reaches of the Yangtze River. Chongqing is also the core of national economic strategies such as the Chengdu–Chongqing Twin Cities Economic Circle and the Western Land–Sea New Corridor. It plays a pivotal role in the economic development and ecological environment protection of the entire Yangtze River basin. Chongqing has a land area of 8.24×10^4 km^2, making it the most prominent mountain city in China. It belongs to the typical category of large cities, large mountainous areas, and large rural areas. The Chongqing Municipal Government has conducted ecological restoration and governance work to address environmental pollution issues. In 2022, the city added 1617 km^2 of water and soil loss control area; the coverage rate of green pest control for major agricultural crops reached 51.76%; and the coverage area of livestock tail water treatment in the city reached 90,000 mu. These efforts have to some extent eased the conflict between economic development and environmental protection (data from the "2022 Chongqing Ecological Environment Status Bulletin" released by the Chongqing Municipal Bureau of Ecology and Environment (https://sthjj.cq.gov.cn, accessed on 10 December 2023). However, with the rapid economic development in the region, the contradictions between agricultural planting, economic growth, and ecological protection will gradually intensify. There are 39 districts and counties and 1035 townships in Chongqing, with complex terrain, a variable climate, multiple soil types, and abundant plant types. It is challenging to solve the problem of ANPSP in identifying districts and counties, and it is tough to prevent and control it in various townships accurately. In addition, due to the complex terrain, variable climate, diverse soil types, and rich planting types in the region, the current ANPSP problem is difficult to control over a large area. Therefore, accurately identifying key control areas is a critical problem that needs to be solved.

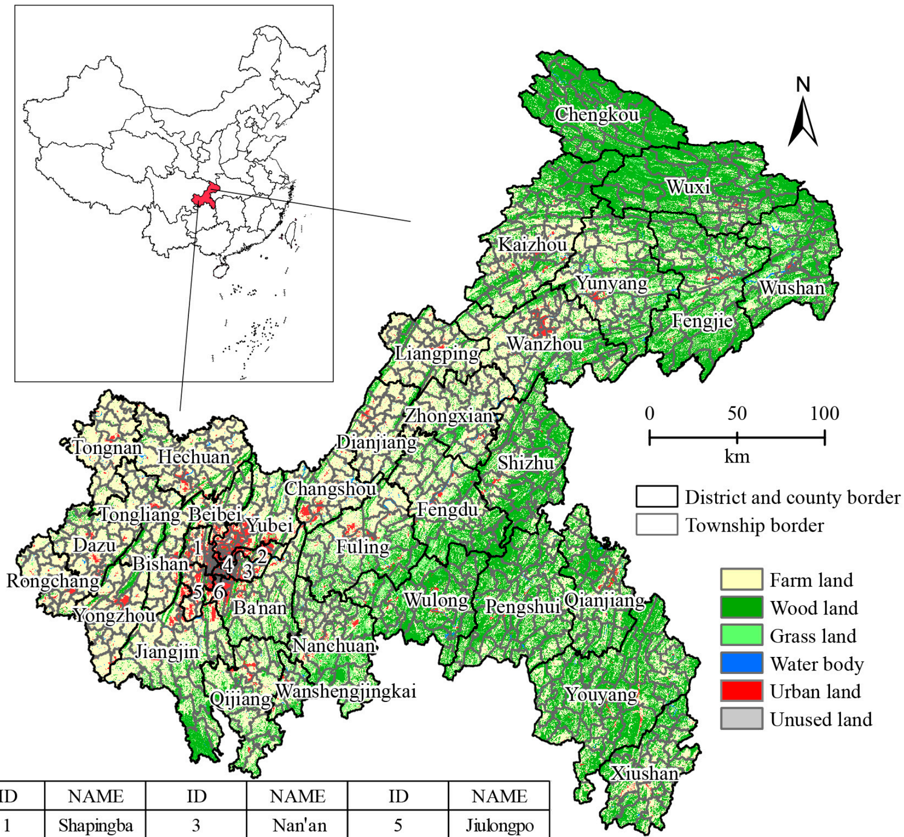

ID	NAME	ID	NAME	ID	NAME
1	Shapingba	3	Nan'an	5	Jiulongpo
2	Jiangbei	4	Yuzhong	6	Dadukou

Figure 1. Location map of Chongqing city.

2.2. Data Sources

The data used in this study mainly include land use data (2000, 2010, and 2020), vegetation coverage index (NDVI) data (from the Resource and Environment Science Data Center of the Chinese Academy of Sciences (http://www.resdc.cn/, accessed on 20 November 2023), digital elevation model (DEM) data (from the Geographic Space Data Cloud of the Chinese Academy of Sciences (http://www.gscloud.cn/, accessed on 15 December 2023), water system data and road data (from OpenStreetMap maps), and district and town boundary data (from the Chongqing Municipal Planning Department).

2.3. Methods

2.3.1. The PLUS Model

The PLUS model is software developed by the High-Performance Spatial Computing Intelligent Laboratory (HPSCIL) of the China University of Geosciences (Wuhan) (https://www.urbancomp.net/archives/plus, accessed on 20 August 2023). The model mainly simulates future land use-type data under different scenarios in the study area by using the rule mining framework (LEAS) based on land expansion analysis and the CA model (CARS) based on a multi-type random seed mechanism [28]. The model considers the complexity and micro-nature of the macro-driving factors of the land use system, thus improving the simulation accuracy of the model. The flowchart for land use simulation in this study is shown in Figure 2.

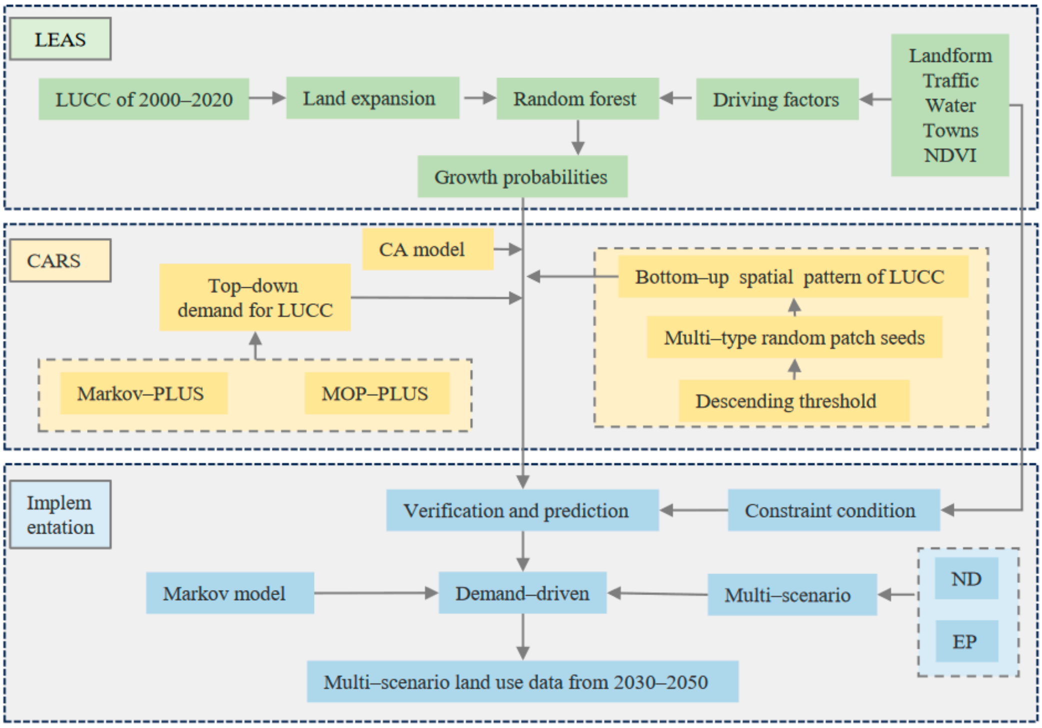

Figure 2. The calculation framework of the PLUS model.

(1) LEAS module.

This module extracts expansion information from the land use data of two periods and uses the random forest classification method to obtain the possibility of growth of each type of land use and the influence weights of each driving factor. The development probability of the spatial point of i land use being converted into k land use is obtained. The specific calculation formula is as follows [22]:

$$P_{i,k}^{d}(x) = \frac{\sum_{n=1}^{M} I(h(x) = d)}{M} \tag{1}$$

In this model, d can be 0 or 1. When d is 1, it means that other land use types are converted to land use type k. When d is 0, it means that land use type k is converted to other land cover types. x is a high-dimensional vector composed of multiple driving factor variables. $I()$ is an indicator function. $h_n(x)$ is the type of element x simulated by the n-th decision tree. M is the total number of decision trees in the random forest model.

(2) CARS module.

This module combines the top-down and bottom-up structural mechanisms, connecting random seed generation with the decreasing threshold. Under the constraints of development probability and the number of land uses, it automatically simulates the generation of land use patches with the following calculation formula [29]:

$$OP_{i,k}^{d=1,t} = \begin{cases} P_{i,k}^{d=1,t} \times (\gamma \times \mu_k) \times D_k^t, \Omega_{i,k}^t = 0 \; and \; \gamma < P_{i,k}^{d=1} \\ P_{i,k}^{d=1} \times \Omega_{i,k}^t \times D_k^t, \Omega_{i,k}^t \neq 0 \; or \; \gamma \geq P_{i,k}^{d=1} \end{cases} \tag{2}$$

In this equation, γ is a random value from 0 to 1. OP represents the total probability of the i-th pixel transitioning from the initial land use type to the k-th land use type in the t-th iteration. μ_k is the threshold for the k-th site type to generate a new patch. D_k^t is the inertia coefficient of the k-th land use type in the t-th iteration. $\Omega_{i,k}^t$ is the spatial influence factor of the i-th pixel transitioning from the initial land use type to the k-th land use type in the t-th iteration.

Land use change is a complex process that varies over time and space. Therefore, the selection of driving factors should consider data availability, security, accessibility, and comprehensiveness. Considering the data availability and human activity impact, the driving factors selected in this study are shown in Table 1.

Table 1. Driving factors and their meanings.

Types	Driving Factors	Meaning
Terrain data	Elevation	DEM data
Traffic data	Distance from highway Distance from expressway Distance from ordinary highways	The distance from roads and water systems is expressed in Euclidean distance
Stream	Distance from other roads Distance from primary rivers Distance from secondary rivers	
Urban data	Urban land	/
Vegetation Index	NDVI data	/
Regions restricted by national regulations for development	Water area	/

Land use needs and development vary across regions. To make the results more scientific and reliable, this study sets up two scenarios to simulate the future land use situation in Chongqing from 2030 to 2050, providing a more reliable and forward-looking scientific and theoretical reference for relevant departments in Chongqing.

Scenario 1: ND: Based on the land use changes in Chongqing from 2000 to 2020, according to the current land use spatial evolution laws, without setting any policy impacts, the land use needs under the natural growth scenario from 2030 to 2050 are predicted with an interval of 10 years.

Scenario 2: EP: Based on the land use changes in Chongqing from 2000 to 2020, urban development will be limited, and the ecological environment will be protected. Combined with the current Chinese farm land protection strategy and the transformation of urban development models, in the EP, the growth rates of farm land, grass land, and unused land are reduced by 10%, and the growth rates of wood land, water bodies, and urban land are reduced by 10% to balance the area changes [30,31].

2.3.2. The Export Coefficient Model

The export coefficient model was proposed to calculate the total pollution load in a watershed under different land use types [32]. The model is based on the mathematical method of multivariate linear regression analysis. Combining the determined pollutant output coefficients and land use data, the model constructs the relationship between land use types and non-point source pollution load values in Chongqing. Then, the pollution load of different types is summed to obtain the total pollution load of the study area. The total pollution load is divided into five levels: low-level zone, lower-level zone, medium-level zone, higher-level zone, and high-level zone, according to the natural breakpoint method. In this study, the total pollution emission was represented by the agricultural emissions of TN and TP. The model equation is as follows [16]:

$$L_j = \sum_{i=1}^{m} E_{ij} A_i + P \tag{3}$$

In this equation, j is the type of pollutant; i is the type of land use in the watershed, with a total of m types; L_j is the total load of pollutant j in the watershed (kg·hm^{-2}·a^{-1}); E_{ij} is the output coefficient of pollutant j in the i-th type of land use in the watershed (kg·hm^{-2}·a^{-1}); A_i is the area of the i-th type of land use (hm^2); P is the total amount of pollutant input by rainfall (kg·hm^{-2}·a^{-1}), which is not considered in this study. Based on existing research and the actual situation of the study area, the output coefficients of each land use type are determined as shown in Table 2 (Currently, the commonly used land use type data does not distinguish between dryland and paddy fields, and Chongqing belongs to a typical dryland and paddy field rotation region. Unused land refers to bare land, wasteland, and other land that cannot be included in the other five types.), concerning the study by Zhu et al. [33].

Table 2. The output coefficient of land use types in Chongqing.

Pollution Type	Farm Land	Wood Land	Grass Land	Urban Land	Water Body	Unused Land
TN	24.19	2.60	6.04	13.00	-	-
TP	1.86	0.17	0.85	1.80	-	-

3. Results

3.1. Land Use Status and Simulation Accuracy Analysis

Chongqing's land use types have undergone significant changes from 2000 to 2020, as shown in Figure 3. The largest land use type is farm land, with its area share decreasing from 46.93% in 2000 to 45.05% in 2020. Urban land area share increased from 608.82 km^2 in 2000 to 2383.76 km^2 in 2020, with a clear increasing trend. This is mainly due to the expansion of cities, which have occupied cultivated land in neighboring areas. Forest area increased first and then decreased; grass land area showed a decreasing trend; and water area showed an increasing trend.

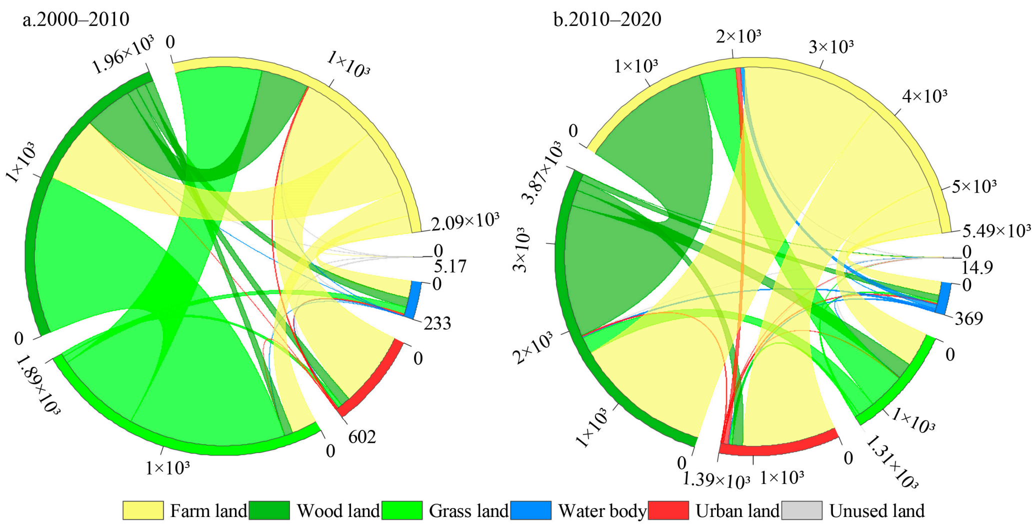

Figure 3. Land transfer matrix from 2000 to 2020 (unit: km^2). (**a**) is the result from 2000 to 2010; (**b**) is the result from 2010 to 2020.

The Kappa coefficient was used to evaluate the accuracy of the PLUS model. The Kappa coefficients of this study's 2000–2010 and 2010–2020 simulations were 0.92 and 0.89, respectively. These values indicate that the simulated results are highly consistent with the actual data, with high simulation accuracy. The model can accurately reflect the land use distribution in the study area. The comparison results are shown in Figure 4.

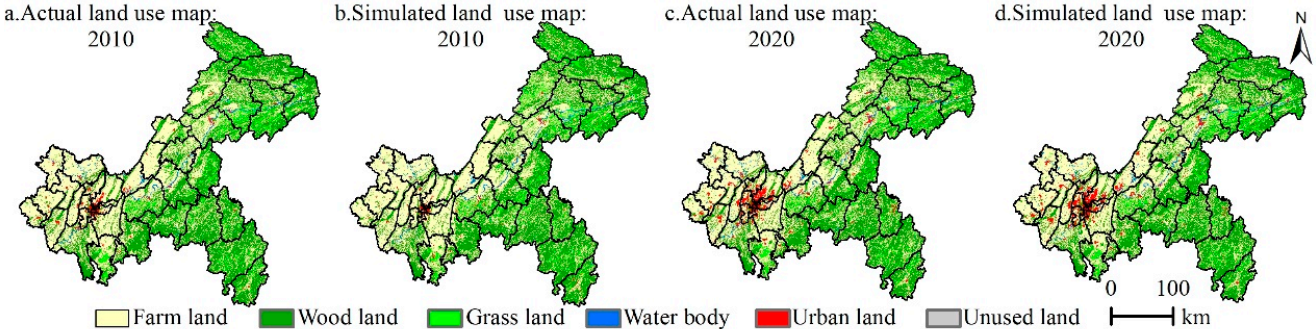

Figure 4. Comparison of simulated and actual land use in Chongqing in 2010 and 2020. (**a**) is the actual land use situation in 2010; (**b**) is the simulated land use situation in 2010; (**c**) is the actual land use situation in 2020; and (**d**) is the simulated land use situation in 2020.

3.2. Land Use Data Simulation under Future Development Scenarios

Based on the land use data of Chongqing in 2020, the PLUS model was used to simulate the area of each land use type under the two scenarios of 2030–2050 and obtain the land use transition matrix, as shown in Figures 5–7.

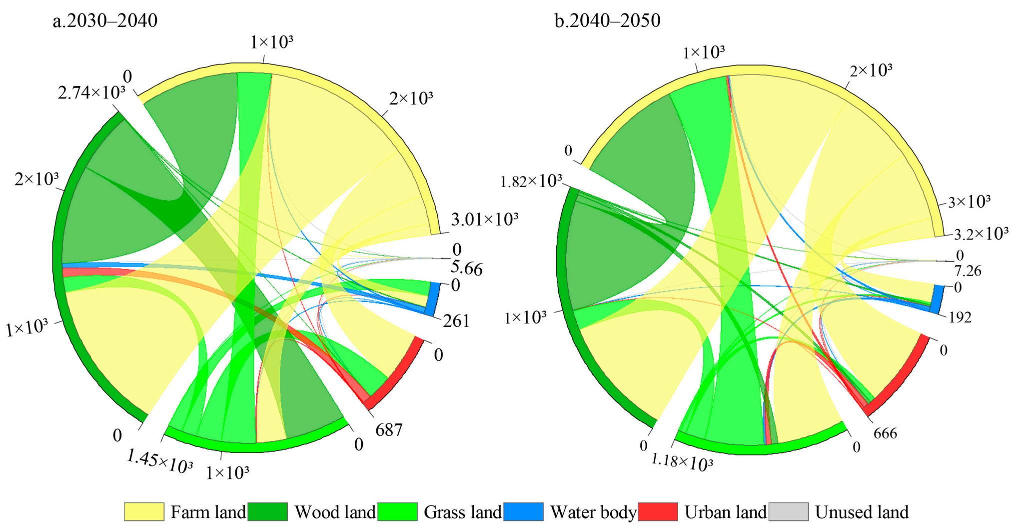

Figure 5. Land use transition matrix under the ND (unit: km^2). (**a**) is the result from 2030 to 2040; (**b**) is the result from 2040 to 2050.

In the two scenarios, farm land and wood land are Chongqing's main land use types. Farm land is mainly distributed in the southwest of the Chongqing metropolitan area and the southwest of the Northeast Chongqing urban agglomeration, while wood land is distributed primarily in the northeast of the Northeast Chongqing urban agglomeration and the northeast of the Southeast Chongqing urban agglomeration. Farm land, grass land, and unused land are decreasing, while wood land, water bodies, and urban land are increasing. In the ND scenario and EP scenario, the area of urban land, water body, and wood land increased by (33.22%, 36.05%), (18.50%, 12.98%), and (0.84%, 0.92%), respectively, in 20 years, with a significant increase in urban land. Farm land, grass land, and unused land decreased by (4.52%, 4.06%), (0.20%, 2.08%), and (2.91%, 6.33%), respectively, in 20 years. Under the two scenarios, urban land is mainly concentrated in the outward expansion of the Chongqing metropolitan area. Grass land mainly grows in the Northeast Chongqing urban agglomeration and the Southeast Chongqing urban agglomeration. Compared with the ND scenario, the EP scenario restricts the probability of land use transfer to a certain extent. The trend of reducing the area of ecological land is effectively controlled, and the reduction rate slows down.

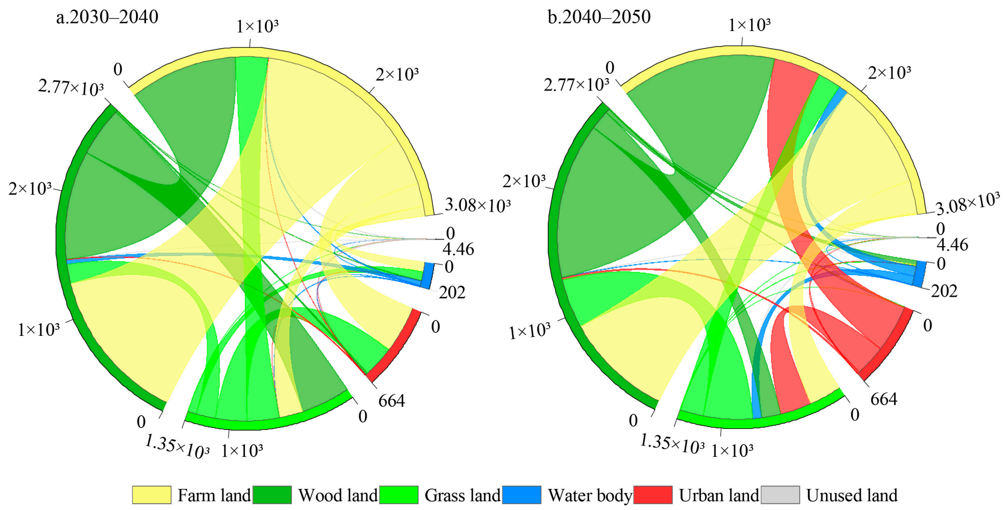

Figure 6. Land use transition matrix under the EP (unit: km^2). (**a**) is the result from 2030 to 2040; (**b**) is the result from 2040 to 2050.

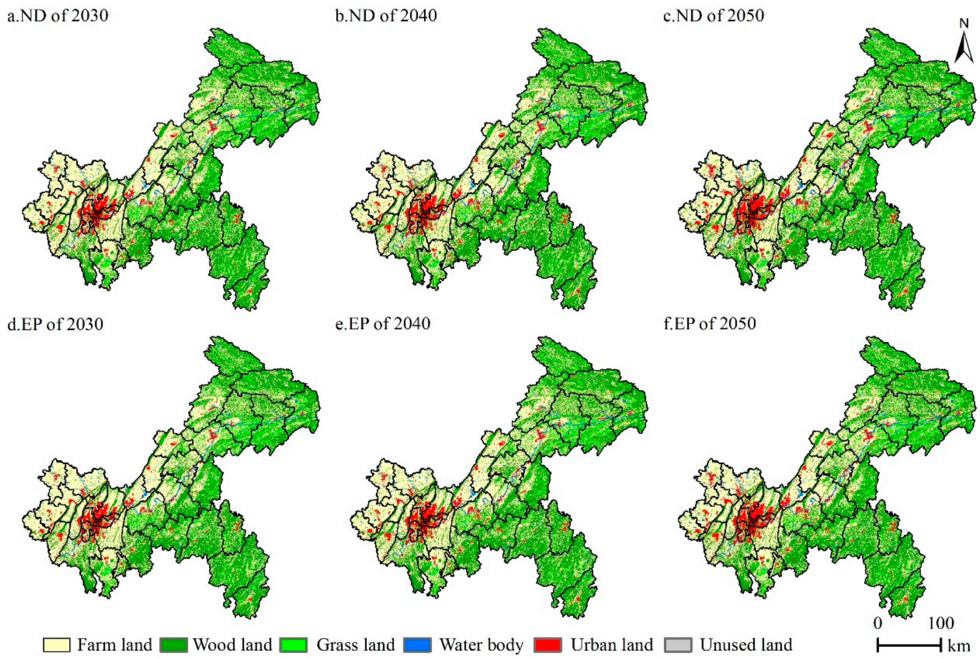

Figure 7. Simulation results of land use types under two development scenarios in 2030–2050. (**a**–**c**) is the result of ND; (**d**–**f**) is the result of EP.

3.3. Measuring ANPSP Load in Long-Term Series

3.3.1. Analysis of Changes in ANPSP Load from 2000 to 2020

From 2000 to 2020, the total pollution load showed a downward trend, but the overall load value was relatively high due to the large base. The total pollution load of TN and TP in 2000, 2010, and 2020 was 1.08×10^8 kg, 1.07×10^8 kg, and 1.05×10^8 kg, and 8.61×10^6 kg, 8.55×10^6 kg, and 8.53×10^6 kg, respectively. The main sources of ANPSP TN and TP from 2000 to 2020 were both farm land, with TN and TP pollution load emissions of 9.31×10^7 kg, 9.23×10^7 kg, and 8.93×10^7 kg, and 7.16×10^6 kg, 7.10×10^6 kg, and 6.87×10^6 kg, respectively. In all cases, the total contribution rate to pollution emissions was over 80%. The contribution rates of wood and grass land to pollution emissions were relatively low, with the average annual contribution rate of TN emissions being 8.09% and 4.68%, respectively, and the average contribution rate of TP emissions being 6.61%

and 8.23%, respectively. The contribution rate of urban land was the lowest, with average contribution rates of 1.69% and 2.92% for TN and TP emissions, respectively.

3.3.2. Analysis of the Change in ANPSP Load under the ND in 2030–2050

In the ND, the total load of TN and TP is reduced, and the distribution of TN and TP pollution load levels is roughly the same, as shown in Figure 8.

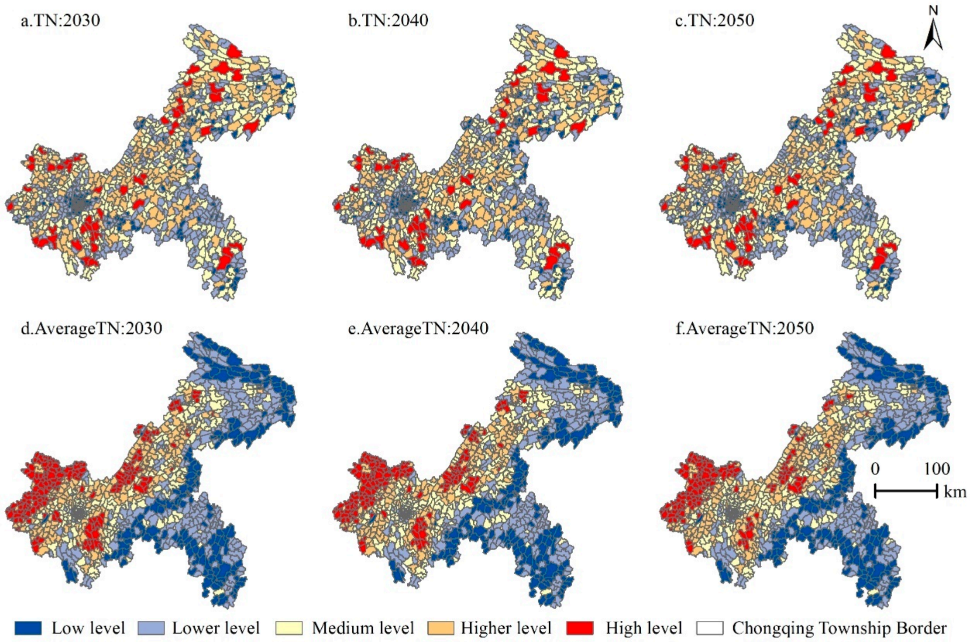

Figure 8. Distribution of average TN and TP load levels for each township under the ND (TP trend is consistent). (**a**–**c**) respectively represent the load situation of TN 2030–2050; (**d**–**f**) respectively represent the average load situation of TN 2030–2050.

From 2030 to 2050, the quantity changes are shown in Table 3. In the TN pollution level, the low levels and high levels remain stable, with an average annual percentage of 20.68% and 4.41%, respectively. The lower-level zone shows an increasing trend, with the percentage of grade numbers in 2030, 2040, and 2050 being 31.88%, 32.17%, and 32.66%, respectively. The medium-level zone shows a fluctuating trend, with the percentage of grade numbers in 2030, 2040, and 2050 being 28.02%, 28.21%, and 27.83%, respectively. The higher-level zone decreases from 15.17% in 2030 to 14.30% in 2050. Among them, there are five towns with an increase of more than 1.00×10^4 kg. The rise of Mawu Town, Fushou Town, Qingyang Town, Zhonggang Township, and Xinglong Town is relatively large, all of which have increased by more than 1.20×10^4 kg. Except for Qingyang Town, which rose by one level, the levels of the remaining areas remain unchanged. There are 72 towns, with a decrease of more than 1.00×10^4 kg. Jiasi Town, Tai'an Town, Youxi Town, Fengming Town, Qiantang Town, Shima Town, and Zitong Street have the largest decrease, all of which have decreased by more than 1.20×10^4 kg, and the load level remains unchanged.

Table 3. Distribution of pollution load levels in the ND from 2030 to 2050.

Pollution Load Level	Number of Townships (TN)			Number of Townships (TP)		
	2030	2040	2050	2030	2040	2050
Low-level zone	211	215	216	229	230	229
Lower-level zone	330	333	338	339	339	346
Medium-level zone	290	292	288	265	226	264
Higher-level zone	157	150	148	147	147	147
High-level zone	47	45	45	55	53	49

From 2030 to 2050, the TP pollution load remained stable in the low-level, lower-level, medium-level, and higher-level zones, with the annual average percentage of grade numbers being 22.16%, 32.98%, 25.60%, and 14.20%, respectively. The high-level zone showed a downward trend, with the number of zones accounting for 5.31%, 5.12%, and 4.73% in 2030, 2040, and 2050, respectively. Among them were three townships with an increase of more than 1.00×10^3 kg, namely Zhonggang Township, Mawu Township, and Fushou Township. The grades remained unchanged. There were 17 townships with a decrease of more than 1.00×10^3 kg, with Shima Township having the largest decrease, but it remained in the high-level zone.

The overall trend of the average load levels of TN and TP distribution is consistent with that from 2000 to 2020. The average load level decreases from west to east, with the highest average load level in the Chongqing metropolitan area and the lowest average pollution load in the Southeast Chongqing urban agglomeration. Among the average load levels in TN, 17 areas were upgraded, 97 areas were downgraded, and 921 areas remained unchanged. The areas with unchanged levels accounted for 88.99%. Among the average load levels of TP, 26 areas were upgraded, 56 areas were downgraded, and 952 areas remained unchanged. The areas with unchanged levels accounted for 91.98%. In particular, the TN and TP loads in Banan District have a clear downward trend. The changes in the high-level zones of the average load level of TN in 2030, 2040, and 2050 are 69.23%, 61.54%, and 46.15%, respectively. The changes in the high-level zones of the average load level of TP in 2030, 2040, and 2050 are 53.85%, 46.15%, and 30.77%, respectively.

3.3.3. Analysis of the Change in ANPSP Load under the EP in 2030–2050

In the EP, the pollution levels of TN and TP are the same. The load levels of all towns tend to be stable from 2030 to 2050, as shown in Figure 9.

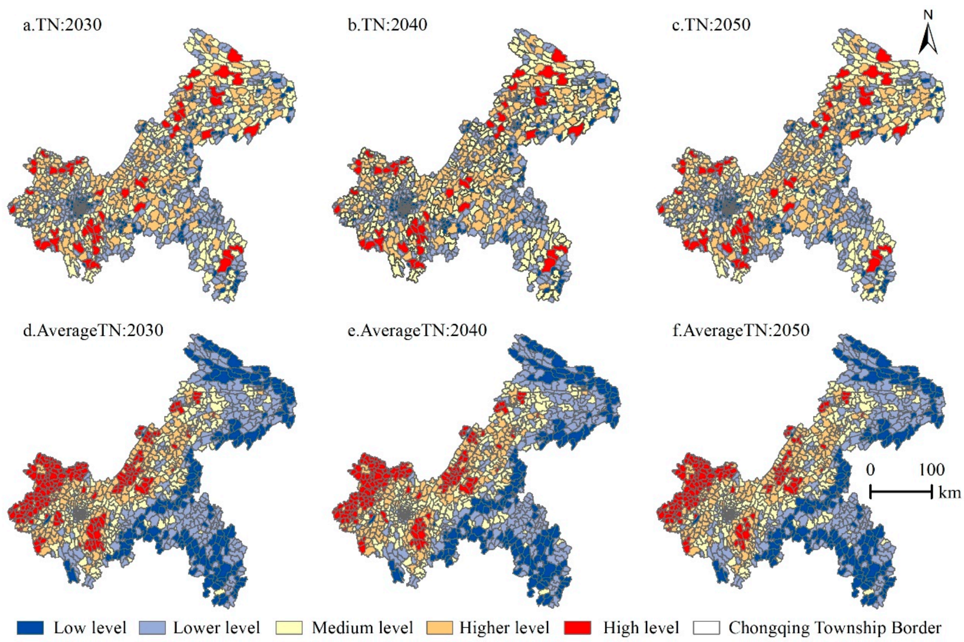

Figure 9. Distribution of average TN and TP load levels for each township under the EP (TP trend is consistent). (**a**–**c**) respectively represents the load situation of TN 2030–2050; (**d**–**f**) respectively represents the average load situation of TN 2030–2050.

From 2030 to 2050, the quantity changes are shown in Table 4. The town with the highest percentage of TN pollution levels is in the lower-level zone, with an average annual rate of 32.20%, which shows a fluctuating trend. The percentage of loads is 31.98% $\rightarrow$ 31.88% $\rightarrow$ 32.75%. The medium-level zone remains stable, with an average annual rate of 28.08%; the low-level zone shows an upward trend; and the high-level zone and the higher-level zone show a downward trend. Among them, there are seven towns with an increase of more than 1.00×10^4 kg, namely, Mawu Town, Fushou Town, Qingyang Town, Zhonggang Township, Xinglong Town, Baitao Street, and Ganzhui Town; the number of towns with a decline of more than 1.00×10^4 kg is 61, and the decrease of Jiasi Town, Zi Tong Street, Youxi Town, and Shima Town is relatively large, all of which are greater than 2.10×10^4 kg.

Table 4. Distribution of pollution load levels in the EP from 2030 to 2050.

Pollution Load Level	Number of Townships (TN)			Number of Townships (TP)		
	2030	2040	2050	2030	2040	2050
Low-level zone	210	215	216	229	230	229
Lower-level zone	331	330	339	341	340	345
Medium-level zone	290	295	287	264	264	264
Higher-level zone	157	150	148	146	148	147
High-level zone	47	45	45	55	53	50

The town with the highest percentage of TP pollution levels is in the lower-level zone, with an average annual rate of 33.04%; only the high-level zone shows a downward trend, with the percentage of loads from 2030 to 2050 being 5.31% → 5.12% → 4.83%. The remaining pollution levels remain stable. Among them, there are only four towns with an increase of more than 1.00×10^3 kg, namely, Zhonggang Township, Fushou Town, Mawu Town, and Baitao Street; the number of towns with a decline of more than 1.00×10^3 kg is 16, with the decline being relatively small, and the town with the largest decline is Shima Town.

The average load level's spatial distribution trend is consistent with the ND. In the TN average load level, 10 towns were upgraded, 107 towns were downgraded, and 918 towns remained the same. In the TP average load level, 7 towns were upgraded, 59 towns were downgraded, and 969 towns remained the same. Among them, the level of Banan District has decreased significantly. In the TN average load, Dongwenquan Town, Huimin Street, and Tianxingsi Town levels have been downgraded to higher-level zones. In the TP average load, Huimin Street and Tianxingsi Town levels have been downgraded to higher-level zones.

3.4. Sensitivity Analysis of Output Coefficients to Pollutant Load Levels

As shown in Figure 10, when the output coefficients of TN and TP are increased by 5% in both scenarios, the townships with an increased pollution load are relatively evenly distributed. When the output coefficients of TN and TP are increased by 10%, the number of townships with an increased pollution load increases significantly, with an average increase of more than 80% per year. When the output coefficients of TN and TP are decreased by 5%, the spatial distribution of townships with decreased pollution load is inconsistent with that of townships with increased pollution load by 5%, and the number of townships with decreased pollution load is relatively small. When the output coefficients of TN and TP are decreased by 10%, the number of townships with a decreased pollution load is less than that of townships with an increased pollution load by 10%. Therefore, when the output coefficients of TN and TP increase, the pollution load increases, and vice versa. When the output coefficients are adjusted, the pollution load levels of all townships change accordingly. In both scenarios, the areas with the most changes in the pollution load levels of townships are the sensitive areas. Specific sensitive areas are shown in Table 5.

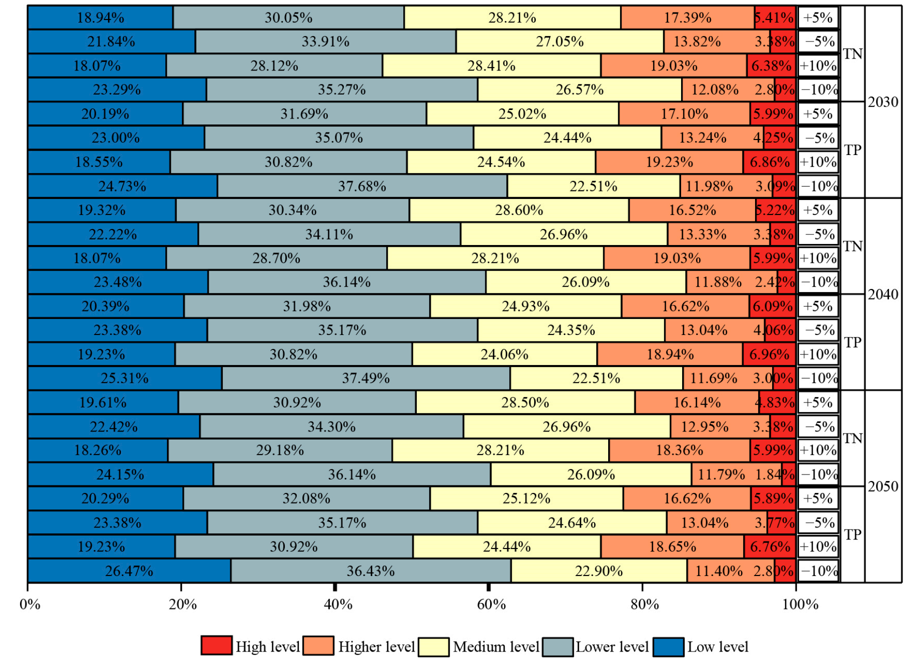

Figure 10. Percentage of TN and TP pollution levels under the ND with changed output coefficients (the trend is consistent under the EP).

Table 5. Regions where load levels are sensitive to farmer behavior in two scenarios for 2030–2050.

	Chongqing Metropolitan Area	Northeast Chongqing Urban Agglomeration	Southeast Chongqing Urban Agglomeration
+5%	Hechuan, Jiangjin, Bishan, and Rongchang	Zhongxian, Liangping, Yunyang, and Fengjie	Wulong and Pengshui
+10%	Hechuan, Nanchuan, Qijiang, Jiangjin, Bishan, Rongchang, and Changshou	Zhongxian, Liangping, Wanzhou, Yunyang, Fengjie, and Wushan	Wulong, Pengshui, and Xiushan
−5%	Dazu and Nanchuan	Fengdu and Kaizhou	Youyang
−10%	Tongliang, Qijiang, Nanuan, Banan, Fuling, Dazu, and Yubei	Fengdu, Dianjiang, Kaizhou, Wanzhou, Fengjie, and Wuxi	Shizhu, Pengshui, and Youyang

4. Discussion

4.1. The PLUS Model Is Suitable for Simulating Land Use-Type Data in Chongqing City

Previous research has shown that the PLUS model has been used for land use change and optimization, ecological risk assessment, and scenario simulation. The model can compensate for the evolutionary ability of land patches under different policies of other models such as FLUS, CLUE-S, and CA-Markov. It is also suitable for simulating regions of larger scales with high simulation accuracy [34]. In this study, we compared our results with those of other studies ([29,34–36]; the specific results are shown in Table 6) and found that our kappa coefficients were 0.92 and 0.89, respectively. This indicates that our simulation accuracy is high, which has certain advantages in accuracy and provides more reference value.

Table 6. Simulation accuracy was studied by other authors.

Author	Model	Study Area	Kappa
Lu et al. [34]	PLUS	The yellow river	0.812
Cao et al. [35]	PLUS	Hefei	0.85
Han et al. [29]	PLUS	Enshi City and Lichuan City	0.81
Li et al. [36]	PLUS	Hangzhou City	0.75

4.2. Sensitivity Analysis Can Better Identify Key Areas for Pollution Control

Identifying critical areas for the control of ANSP is essential to improving the cost-effectiveness of regional protection practices [37,38]. Most existing studies have identified critical areas based on the "amount" of pollution load. For example, Ding et al. [39] used the SWAT model to identify key source areas based on the control units; Chang et al. [40] identified key pollution source areas in the study area based on nutrient load and nutrient load intensity, which is a method to identify critical control areas based on the average pollution load of TN and TP; and Xu et al. [41] identified key control source areas based on the size of the comprehensive pollution index.

In this study, we can identify areas with a high pollution load and key areas for control in the study area by adjusting the output coefficients to achieve sensitivity analysis. This can more clearly identify areas more sensitive to changes in output coefficients. As the output coefficients are increased, the number of sensitive areas increases. Therefore, control over sensitive areas should be strengthened.

4.3. Land Use Pattern Optimization Plays an Important Role in the Prevention and Control of ANPSP

In this study, we analyzed the proportion of townships with a land use structure of more than 20%, 40%, 60%, and 80% of cultivated land and forest land in 2020 and 2050, as well as the proportion of the total pollution load of these townships in the total pollution load of all townships. The results are shown in Table 7. The results show that the total pollution load mainly comes from farm land and wood land. However, even when the proportion of farm land is low, the pollution load of the township is still high. The pollution load of townships with more than 80% wood land is extremely low. This shows that the land use structure significantly impacts the pollution load. In both scenarios, the total pollution load of farm land and wood land in the EP is relatively low. This shows that optimizing land use structure is beneficial to reducing the pollution load.

Table 7. Share of farm land, wood land, and total pollution level proportion (unit: %).

			20%		40%		60%		80%	
			Township	**Total Pollution Level**	**Township**	**Total Pollution Level**	**Township**	**Total Pollution Level**	**Township**	**Total Pollution Level**
2020		Farm land	83.86	93.00	52.27	64.25	31.69	42.31	15.17	21.17
2020		Wood land	62.80	63.54	38.55	36.24	18.55	15.37	2.71	1.55
2050	NP	Farm land	81.06	91.67	46.86	59.52	27.54	37.35	10.92	15.73
2050	NP	Wood land	64.15	66.16	39.13	38.34	19.13	16.72	2.61	1.48
2050	EP	Farm land	80.87	91.61	45.99	58.63	27.05	36.45	10.72	15.38
2050	EP	Wood land	64.25	66.13	39.13	38.21	19.13	16.64	2.71	1.44

Existing studies by Zhu [42], Lin [30], and Han [29] et al. have shown that the ecological protection scenario is conducive to pollution control or the improvement of environmental risk through multi-scenario simulation of point source pollution.

4.4. Limitations and Future Prospects of this Study

This study can provide methods and data support for ANPSP control in Chongqing. However, this study still has some shortcomings. First, the driving factors considered in the simulation of land use type data are currently commonly used but may also be incomplete. Second, the selection of output coefficients in calculating the ANPSP load mainly refers to the existing research results, which may differ from the actual situation. This study's farm land output coefficient did not distinguish between dryland and paddy fields and will be further considered in the future. Third, this study did not conduct an in-depth analysis of the influencing factors of the ANPSP load. Therefore, in the future, we will conduct in-depth research on relevant topics, obtain more localized parameters, and identify the key influencing factors of ANPSP load to effectively support the goal of regional agricultural green development and the construction of a beautiful China.

5. Conclusions

This study uses a combination of the PLUS model and the output coefficient model to analyze the evolution trend of ANPSP load for a long time series from 2000 to 2050 in Chongqing. It also analyzes the sensitivity of regional pollution loads to output coefficient adjustment. This study provides good data and methodological support for regional agricultural green development and constructing a beautiful China. The main conclusions are as follows:

(1) The PLUS model has high accuracy in simulating the spatial distribution of future land in Chongqing. Wood land and farm land are the primary land use types in Chongqing. In the ND, the urban land area will increase from 3.98% in 2030 to 6.20% in 2050. In the EP, the urban land area will increase from 3.87% in 2030 to 5.87% in 2050. The urban expansion will further occupy cropland.

(2) From 2000 to 2020, the proportion of high-level zones with TN pollution load levels in Chongqing was 4.93%, 5.02%, and 4.73%, respectively. In both scenarios, the number of high-level zones decreased, and the average load level decreased from west to east.

(3) The sensitivity analysis found that the number of townships with increased levels when TN and TP output coefficients were increased was greater than the number of townships with decreased levels when the output coefficients were decreased. This indicates that the risk level is more sensitive to the increase in fertilizer application. Sensitivity analysis can better identify critical areas for pollution control, and the areas sensitive to changes in farmers' behavior mainly include Hechuan District, Nanchuan District, Qijiang District, Jiangjin District, and Bishan District.

Author Contributions: Conceptualization, K.Z., D.G. and Y.H.; methodology, K.Z. and X.T.; software, K.Z., Y.H. and L.Z.; validation, K.Z., X.T. and S.Z.; formal analysis, K.Z. and S.Z.; investigation, K.Z., L.Z. and D.G.; resources, K.Z. and S.Z.; data curation, K.Z. and Y.H.; writing—original draft preparation, K.Z. and Y.Z.; writing—review and editing, K.Z., Y.Z., S.Z. and X.T.; visualization, K.Z. and X.T.; supervision, K.Z. and S.Z.; project administration, K.Z., X.T. and S.Z.; funding acquisition, K.Z., X.T. and S.Z. All authors have read and agreed to the published version of the manuscript.

Funding: This research was supported and funded by the Chongqing Municipal Bureau of Science and Technology (no. CSTB2022TIAD-KPX0120; no. CSTB2022NSCQ-MSX0538), the National Natural Science Foundation of China Youth Science Fund Project (No. 42301353), and the Chongqing Municipal Education Commission (No. 22SKGH569). This work was also supported by the Innovation Center for Green Intelligent Environmental Protection Technology and Equipment Technology in Chongqing and the Chongqing Key Laboratory of Spatial and Temporal Information in Mountainous Cities.

Data Availability Statement: Dataset available on request from the authors.

Conflicts of Interest: The authors declare no conflicts of interest.

References

1. Falconer, L.; Telfer, T.C.; Ross, L.G. Modelling seasonal nutrient inputs from non-point sources across large catchments of importance to aquaculture. *Aquaculture* **2018**, *495*, 682–692. [CrossRef]
2. Chen, T.; Lu, J.Y.; Lu, T.; Yang, X.D.; Zhong, Z.; Feng, H.J.; Wang, M.Z.; Yin, J. Agricultural non-point source pollution and rural transformation in a plain river network: Insights from Jiaxing city, China. *Environ. Pollut.* **2023**, *333*, 121953. [CrossRef] [PubMed]
3. Zhao, H.; Wang, Y.; Dong, Y.K.; He, Z.L.; Wang, P.; Zheng, H.G.; He, J.F.; Zeng, W.J. Modeling the response of agricultural non-point source pollution to planting structure and fertilization level in Erhai Lake Basin under low-latitude plateau climate. *Ecol. Indic.* **2023**, *154*, 110829. [CrossRef]
4. Volk, M.; Liersch, S.; Schmidt, G. Towards the implementation of the European Water Framework Directive?: Lessons learned from water quality simulations in an agricultural watershed. *Land Use Policy* **2009**, *26*, 580–588. [CrossRef]
5. Kumar, L.; Kumari, R.; Kumar, A.; Tunio, I.A.; Sassanelli, C. Water Quality Assessment and Monitoring in Pakistan: A Comprehensive Review. *Sustainability* **2023**, *15*, 6246. [CrossRef]
6. Ahn, S.-R.; Kim, S.-J. The Effect of Rice Straw Mulching and No-Tillage Practice in Upland Crop Areas on Nonpoint-Source Pollution Loads Based on HSPF. *Water* **2016**, *8*, 106. [CrossRef]

7. Zeng, F.F.; Zuo, Z.; Mo, J.C.; Chen, C.Y.; Yang, X.J.; Wang, J.J.; Wang, Y.; Zhao, Z.Q.; Chen, T.Y.; Li, Y.T.; et al. Runoff Losses in Nitrogen and Phosphorus From Paddy and Maize Cropping Systems: A Field Study in Dongjiang Basin, South China. *Front. Plant Sci.* **2021**, *12*, 675121. [CrossRef] [PubMed]
8. Wang, M.M.; Jiang, T.H.; Mao, Y.B.; Wang, F.J.; Yu, J.; Zhu, C. Current Situation of Agricultural Non-Point Source Pollution and Its Control. *Water Air Soil Pollut.* **2023**, *234*, 471. [CrossRef]
9. Chuan, L.M.; Zheng, H.G.; Wang, A.L.; Zhao, J.J.; Yan, Z.H. The situation and research progress of agricultural non-point source pollution in China. *IOP Conf. Ser. Earth Environ. Sci.* **2020**, *526*, 012015. [CrossRef]
10. Zhou, L.L.; Geng, R.Z. Development and Assessment of a New Framework for Agricultural Nonpoint Source Pollution Control. *Water* **2021**, *13*, 3156. [CrossRef]
11. Yu, W.Q.; Zhang, J.; Liu, L.J.; Li, Y.; Li, X.Y. A source-sink landscape approach to mitigation of agricultural non-point source pollution: Validation and application. *Environ. Pollut.* **2022**, *314*, 120287. [CrossRef] [PubMed]
12. Park, M.; Choi, Y.S.; Shin, H.J.; Song, I.; Yoon, C.G.; Choi, J.D.; Yu, S.J. A Comparison Study of Runoff Characteristics of Non-Point Source Pollution from Three Watersheds in South Korea. *Water* **2019**, *11*, 966. [CrossRef]
13. Zhang, X.Q.; Chen, P.; Dai, S.N.; Han, Y. Analysis of non-point source nitrogen pollution in watersheds based on SWAT model. *Ecol. Indic.* **2022**, *138*, 108881. [CrossRef]
14. Wang, H.; Liu, C.; Xiong, L.C.; Wang, F.T. The spatial spillover effect and impact paths of agricultural industry agglomeration on agricultural non-point source pollution: A case study in Yangtze River Delta, China. *J. Clean. Prod.* **2023**, *401*, 136600. [CrossRef]
15. Li, N.; Han, W.Z.; Shen, M.N.; Yu, S.L. Load evaluation of non-point source pollutants from reservoir based on export coefficient modeling. *Nongye Gongcheng Xuebao/Trans. Chin. Soc. Agric. Eng.* **2016**, *32*, 224–230. [CrossRef]
16. Johnes, P.J. Evaluation and management of the impact of land use change on the nitrogen and phosphorus load delivered to surface waters: The export coefficient modelling approach. *J. Hydrol. Amst.* **1996**, *183*, 323–349. [CrossRef]
17. Worrall, F.; Burt, T.P.; Howden, N.J.K.; Whelan, M.J. The fluvial flux of nitrate from the UK terrestrial biosphere—An estimate of national-scale in-stream nitrate loss using an export coefficient model. *J. Hydrol.* **2012**, *414–415*, 31–39. [CrossRef]
18. Zhang, L.; Endreny, T.A.; Stephan, E.A. Stochastic export coefficient model to predict annual variation in phosphorus loading from diffuse runoff. *J. Hydrol.* **2023**, *620*, 129447. [CrossRef]
19. Zhu, K.W.; Chen, Y.C.; Xiong, H.L.; Zhang, S.; Yang, Z.M.; Huang, L.; Lei, B. Impact analysis ofthe future development scenario on risks from agricultural non-point source pollution. *J. Agro-Environ. Sci.* **2021**, *40*, 1971–1981.
20. Babbar, D.; Areendran, G.; Sahana, M.; Sarma, K.; Raj, K.; Sivadas, A. Assessment and prediction of carbon sequestration using Markov chain and InVEST model in Sariska Tiger Reserve, India. *J. Clean. Prod.* **2021**, *278*, 123333. [CrossRef]
21. Islam, S.; Li, Y.C.; Ma, M.G.; Chen, A.X.; Ge, Z.X. Simulation and Prediction of the Spatial Dynamics of Land Use Changes Modelling Through CLUE-S in the Southeastern Region of Bangladesh. *J. Indian Soc. Remote Sens.* **2021**, *49*, 2755–2777. [CrossRef]
22. Liang, X.; Guan, Q.F.; Clarke, K.C.; Liu, S.S.; Wang, B.Y.; Yao, Y. Understanding the drivers of sustainable land expansion using a patch-generating land use simulation (PLUS) model: A case study in Wuhan, China. *Comput. Environ. Urban Syst.* **2021**, *85*, 101569. [CrossRef]
23. Blissag, B.; Yebdri, D.; Kessar, C. Spatiotemporal change analysis of LULC using remote sensing and CA-ANN approach in the Hodna basin, NE of Algeria. *Phys. Chem. Earth* **2024**, *133*, 103535. [CrossRef]
24. Chasia, S.; Olang, L.O.; Sitoki, L. Modelling of land-use/cover change trajectories in a transboundary catchment of the Sio-Malaba-Malakisi Region in East Africa using the CLUE-s model. *Ecol. Model.* **2023**, *476*, 110256. [CrossRef]
25. Zhu, K.W.; Yang, Z.M.; Huang, L.; Chen, Y.C.; Zhang, S.; Xiong, H.L.; Wu, S.; Lei, B. Coupling ITO3dE model and GIS for spatiotemporal evolution analysis of agricultural non-point source pollution risks in Chongqing in China. *Sci. Rep.* **2021**, *11*, 4635. [CrossRef]
26. Xiao, X.C.; Ni, J.P.; He, B.H.; Xie, D.T. Estimation of Agricultural Nonpoint Source Pollution Loads and Its Regional Differentiation in Chong. *J. Basic Sci. Eng.* **2014**, *22*, 634–646.
27. Guan, X.Y.; Tao, Y.; Chen, H.R.; Chang, X.M. Assessing risk and governing of agricultural non-point source pollution in Three Gorges Reservoir Areas. *Trans. CSAE* **2023**, *39*, 200–210.
28. Li, X.; Fu, J.Y.; Jiang, D.; Lin, G.; Cao, C.L. Land use optimization in Ningbo City with a coupled GA and PLUS model. *J. Clean. Prod.* **2022**, *375*, 134004. [CrossRef]
29. Han, P.; Xiang, J.W.; Zhao, Q.L. Spatial differentiation and scenario simulation of cultivated land in mountainous areas of Western Hubei, China: A PLUS model. *Environ. Sci. Pollut. Res. Int.* **2023**, *30*, 52804–52817. [CrossRef]
30. Lin, X.; Wang, Z.T. Landscape ecological risk assessment and its driving factors of multi-mountainous city. *Ecol. Indic.* **2023**, *146*, 109823. [CrossRef]
31. Xiang, S.J.; Wang, Y.; Deng, H.; Yang, C.M.; Wang, Z.F.; Gao, M. Response and multi-scenario prediction of carbon storage to land use/cover change in the main urban area of Chongqing, China. *Ecol. Indic.* **2022**, *142*, 109205. [CrossRef]
32. Norvell, W.A.; Frink, C.R.; Hill, D.E. Phosphorus in Connecticut lakes predicted by land use. *Proc. Natl. Acad. Sci. USA* **1979**, *76*, 5426–5429. [CrossRef]
33. Zhu, K.W.; Song, D.; Chen, Y.C.; Huang, C.Q.; Duan, Q.Y.; Zhang, S. Evolution Analysis of Non-point Source Pollution Risk in Chongqing Based on Improved Output Coefficient Model. *Environ. Impact Assess.* **2022**, *44*, 79–83.
34. Lu, C.; Qi, X.; Zheng, Z.S.; Jia, K. PLUS-Model Based Multi-Scenario Land Space Simulation of the Lower Yellow River Region and Its Ecological Effects. *Sustainability* **2022**, *14*, 6942. [CrossRef]

35. Cao, X.F.; Liu, Z.S.; Li, S.J.; Gao, Z.J. Integrating the Ecological Security Pattern and the PLUS Model to Assess the Effects of Regional Ecological Restoration: A Case Study of Hefei City, Anhui Province. *Int. J. Environ. Res Public Health* **2022**, *19*, 6640. [CrossRef] [PubMed]
36. Li, Y.H.; Yao, S.; Jiang, H.Z.; Wang, H.R.; Ran, Q.C.; Gao, X.Y.; Ding, X.Y.; Ge, D.D. Spatial-Temporal Evolution and Prediction of Carbon Storage: An Integrated Framework Based on the MOP–PLUS–InVEST Model and an Applied Case Study in Hangzhou, East China. *Land* **2022**, *11*, 2213. [CrossRef]
37. Huang, J.J.; Lin, X.J.; Wang, J.H.; Wang, H. The precipitation driven correlation based mapping method (PCM) for identifying the critical source areas of non-point source pollution. *J. Hydrol.* **2015**, *524*, 100–110. [CrossRef]
38. Zuo, D.P.; Han, Y.A.; Gao, X.X.; Ma, G.W.; Xu, Z.X.; Bi, Y.Q.; Abbaspour, K.C.; Yang, H. Identification of priority management areas for non-point source pollution based on critical source areas in an agricultural watershed of Northeast China. *Environ. Res.* **2022**, *214*, 113892. [CrossRef] [PubMed]
39. Ding, Y.; Dong, F.; Zhao, J.Y.; Peng, W.Q.; Chen, Q.C.; Ma, B. Non-Point Source Pollution Simulation and Best Management Practices Analysis Based on Control Units in Northern China. *Int. J. Environ. Res. Public Health* **2020**, *17*, 868. [CrossRef]
40. Chang, D.; Lai, Z.Q.; Li, S.; Li, D.; Zhou, J. Critical source areas' identification for non-point source pollution related to nitrogen and phosphorus in an agricultural watershed based on SWAT model. *Environ. Sci. Pollut. Res. Int* **2021**, *28*, 47162–47181. [CrossRef]
41. Xu, W.; Liu, L.; Zhu, S.J.; Sun, A.H.; Ding, Z.Y.; Wang, H. Identifying the critical areas and primary sources for agricultural nonpoint source pollution management of an emigrant town within the Three Gorges reservoir area. *Environ. Monit. Assess.* **2023**, *195*, 602. [CrossRef] [PubMed]
42. Zhu, K.W.; Chen, Y.C.; Zhang, S.; Yang, Z.M.; Huang, L.; Li, L.; Lei, B.; Zhou, Z.B.; Xiong, H.L.; Li, X.X.; et al. Output risk evolution analysis of agricultural non-point source pollution under different scenarios based on multi-model. *Glob. Ecol. Conserv.* **2020**, *23*, e01144. [CrossRef]